Inorganica Chimica Acta, 21 (1977) 119–131

Electronic Structure, Electronic Spectra and Mössbauer Hyperfine Interactions in Ruthenium Complexes

D. GUENZBURGER, A. GARNIER* and J. DANON

Centro Brasileiro de Pesquisas Físicas, Rio de Janeiro, Brasil

and

**Département de Recherches Physiques, Laboratorie associé au C.N.R.S. No. 71, Université Pierre et Marie Curie, Paris, France*

and

UER de Médecine et Biologie Humaine, Université de Paris XIII, Bobigny, France

Received June 12, 1976

Self-consistent charge and configuration molecular orbital calculations have been performed for $[Ru(CN)_6]^{-4}$, $[Ru(NH_3)_6]^{+2}$, $[Ru(NH_3)_6]^{+3}$, $[Ru(CN)_5NO]^{-2}$, $[RuCl_5NO]^{-2}$ *and* $[Ru(NH_3)_5NO]^{+3}$. *The empirical parameters required in the SCCC–MO calculations were derived from the fitting of calculated electronic transitions to those measured by optical absorption spectroscopy. The electronic populations obtained in this manner were used to interpret the isomer shifts and quadrupole splittings measured by Mössbauerspectroscopy with* ^{99}Ru *complexes.*

Introduction

Among the large number of covalent complexes containing Ruthenium as the central atom synthesized up to date, many contain ligands such as CN, CO, NO *etc.* which are known to have low energy π-antibonding orbitals [1]. These orbitals may become populated through bonding with the metal d orbitals; this mechanism, known as back-donation, is particularly striking for the ligand NO [2].

Back-donation and other characteristics of the chemical bond in transition metal complexes may be detected through hyperfine interactions measured by Mössbauer spectroscopy [3]. Isomer shifts and electric quadrupole splittings have been measured for a number of Ruthenium complexes, and the general trends in the results explained by discussing the covalent character of the different metal–ligand bonds involved [4–6]

Further insight into the hyperfine interactions of these complexes requires better knowledge of their electronic structure. For this purpose, we have performed Molecular Orbital calculations for the complex ions $[Ru(CN)_6]^{-4}$, $[Ru(NH_3)_6]^{+2}$, $[Ru(NH_3)_6]^{+3}$, $[Ru(CN)_5NO]^{-2}$, $[RuCl_5NO]^{-2}$ and $[Ru(NH_3)_5NO]^{+3}$, using the semi-empirical SCCC–MO ("self-consistent charge and configuration molecular orbitals") method of Ballhausen and Gray [7]. Preliminary results were reported [8] for $[Ru(CN)_5NO]^{-2}$, $[RuCl_5NO]^{-2}$ and $[Ru(NH_3)_5NO]^{+3}$. M.O. calculations with the CNDO ("complete neglect of differential overlap") method were also reported recently for these complexes [9].

Electronic structure determinations by semi-empirical methods involve approximations which make it difficult to expect them to account for such small effects as the hyperfine interactions. Nevertheless, it would be interesting to verify if semi-empirical M.O. results obtained in such a way as to adequately describe a different molecular property, for example electronic transitions, can be useful in the interpretation of such interactions. With this in view, we have chosen the empirical parameters required in our calculations with the SCCC–MO method by approximately fitting calculated electronic transtions to those measured experimentally by optical spectroscopy of the complexes in solution. Electronic populations obtained in this manner were then used to interpret Mössbauer isomer shifts and quadrupole splittings.

Experimental

The sodium and potassium derivatives of $[Ru(CN)_5NO]^{2-}$ are highly insoluble in water. We have prepared the soluble salt $Li_2[Ru(CN)_5NO]$ by the following procedure: $K_4[Ru(CN)_6]$ was dissolved in hot concentrated HNO_3 during twelve hours. The reaction products are then neutralised with a $LiCO_3$ solution. By adding $AgNO_3$ solution the $Ag_2[Ru(CN)_5NO]$ complex is precipated. After being filtered and washed the silver complex is stirred in a LiCl solution giving AgCl precipitate and the $Li_2[Ru(CN)_5$-

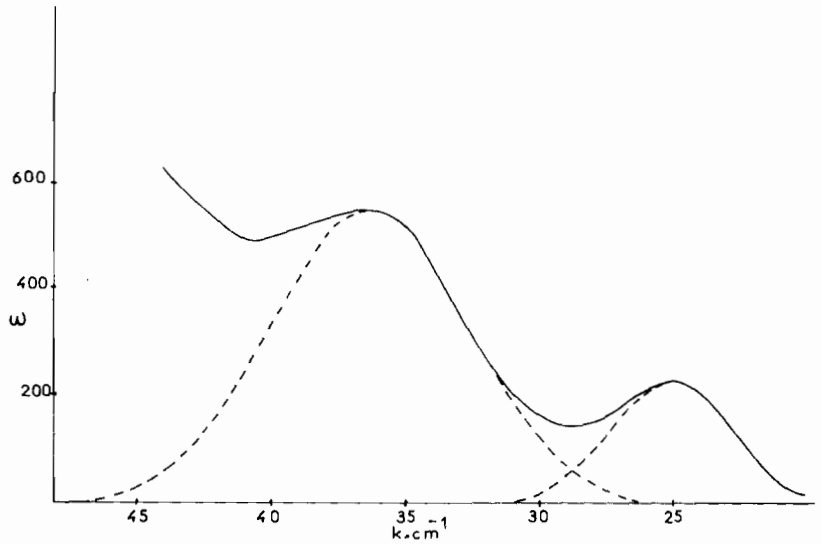

Figure 1. —— Absorption spectra of $[Ru(NH_3)_6]^{2+}$. ---- Gaussian analysis.

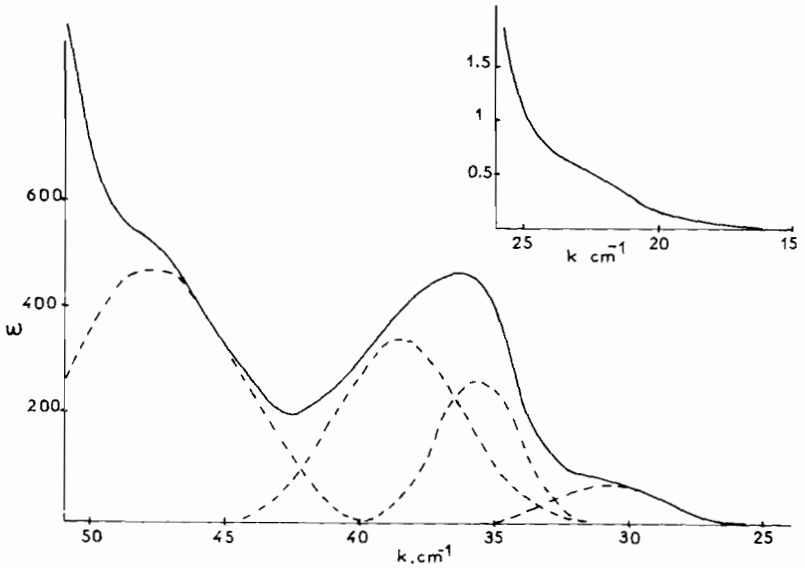

Figure 2. —— Absorption spectra of $[Ru(NH_3)_6]^{3+}$. ---- Gaussian analysis.

NO] in the aqueous solution. From slow evaporation red crystals are obtained from this solution.

$[Ru(NH_3)_6]Cl_2$ and $[Ru(NH_3)_6]Cl_3$ were kindly made available by Dr. U. Wagner from Technische Universität München. Samples of $K_2[RuCl_5NO]$ and $[Ru(NH_3)_5NO]Cl_2$ were prepared by Professor J. P. Mathieu from Département de Recherches Physiques, Paris, according to references 10 and 11.

The electronic spectra of $[Ru(NH_3)_6]^{+2}$ and $[Ru(NH_3)_6]^{+3}$ in solution are presented in Figures 1 and 2. The spectra of $[Ru(CN)_5NO]^{-2}$, $[RuCl_5NO]^{-2}$ and $[Ru(NH_3)_5NO]^{+3}$ are presented in Figures 3, 4 and 5.

A Cary 14 spectrophotometer was used in all cases; the region of absorption scanned ranged from 15 to $\cong$52 kcm^{-1}, and the spectra were analysed by Gaussian decomposition, through a Dupont de Nemours curve analyser. All spectra were taken at room temperature in aqueous solution, except that of unstable $[Ru(NH_3)_6]^{+2}$, which was measured in aqueous solution of NH_3 and nitrogen atmosphere in an attempt to delay decomposition.

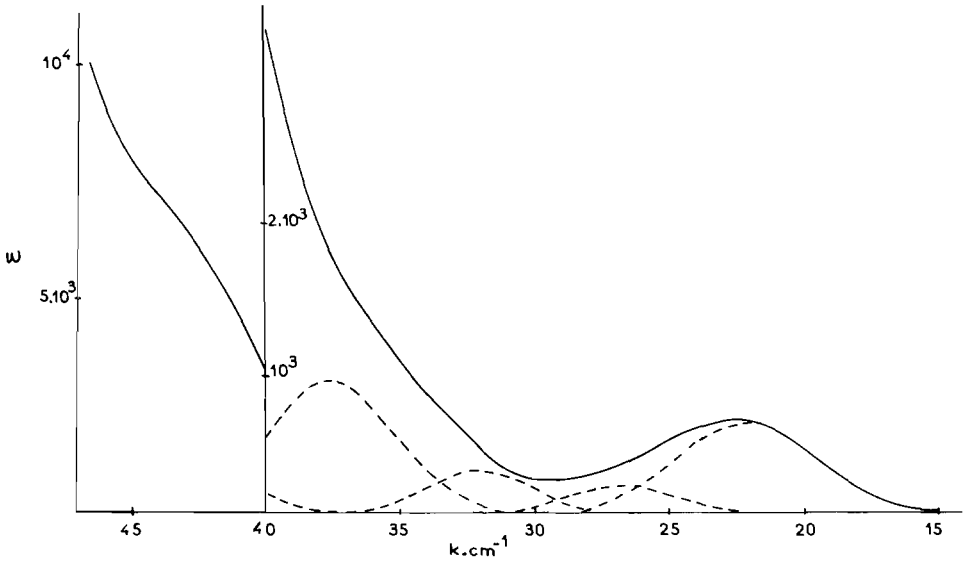

Figure 3. —— Absorption spectra of $[Ru(CN)_5NO]^{2-}$. ----- Gaussian analysis.

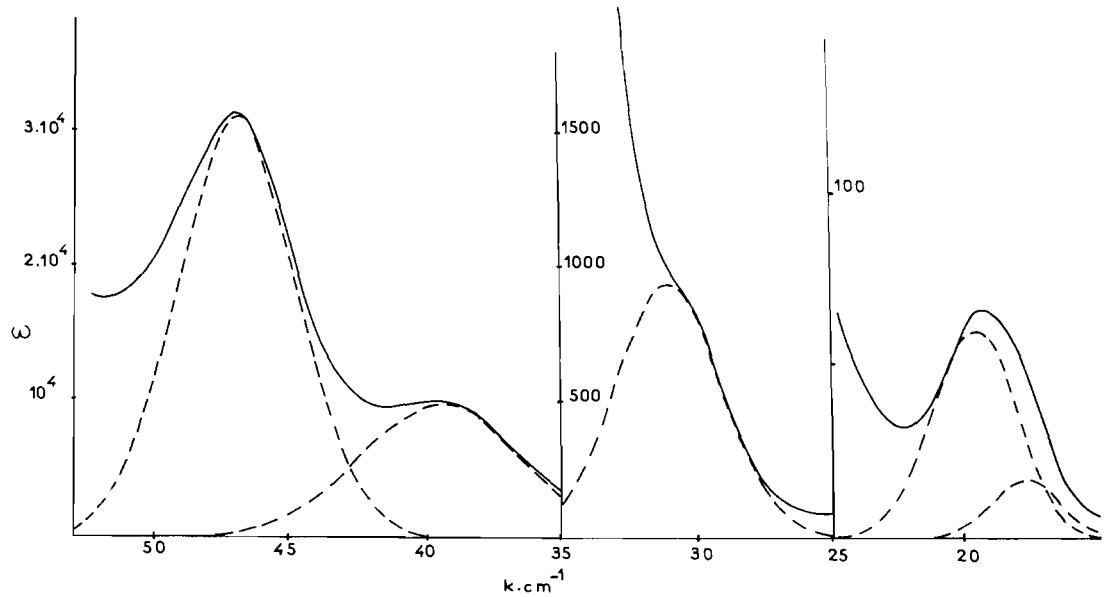

Figure 4. —— Absorption spectra of $[RuCl_5NO]^{2-}$. ----- Gaussian analysis.

Details of the Calculations

The SCCC–MO method was used, as described elsewhere [7]. Non-diagonal elements H_{ij} of the energy matrixes were approximated as

$$H_{ij} = -FG_{ij}\,(H_{ii} \cdot H_{jj})^{1/2}$$

where G_{ij} are the group overlap integrals and F an empirical parameter to be adjusted. Mulliken population analysis [12] were performed. Ligand–ligand overlap corrections were included.

Interatomic distances were taken from X-ray diffraction measurements when available, otherwise they were estimated. Distances in $[Ru(CN)_5NO]^{-2}$, for which C_{4v} symmetry was considered, were estimated by interpolation of values known for analogous complexes of Cr, Mo, Mn and Fe [13]. They are: Ru–CN = 1.95 Å, Ru–NO = 1.75 Å, C–N = 1.16 Å and N–O = 1.13 Å. The same values for Ru–CN and C–N distances were used for $[Ru(CN)_6]^{-4}$ (O_h symmetry). Interatomic distances available in the literature for $[RuCl_5NO]^{-2}$ were used [14]. These

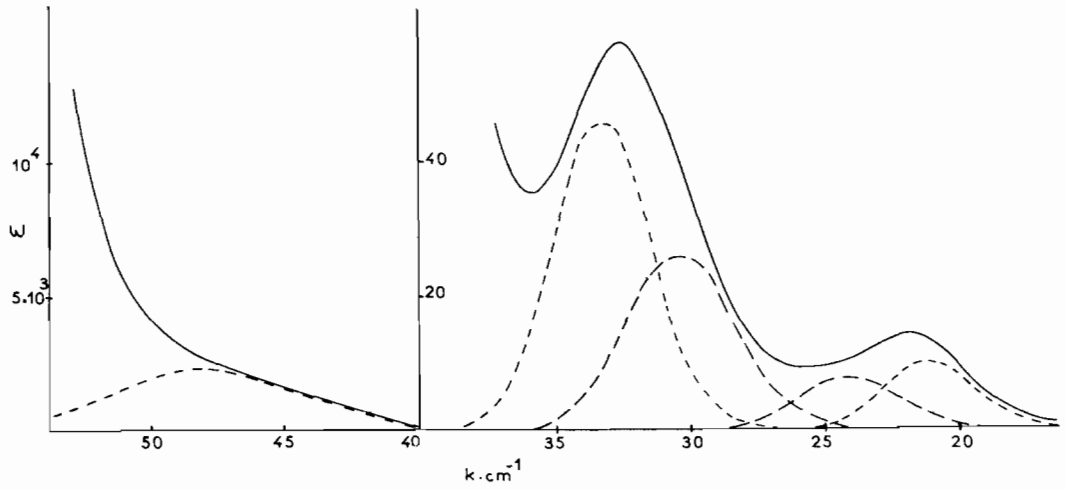

Figure 5. —— Absorption spectra of $[Ru(NH_3)_5NO]^{3+}$. ---- Gaussian analysis.

are Ru–N = 1.79 Å, Ru–Cl = 2.36 Å, N–O = 1.08 Å. In spite of the deviation from 180 ° reported for the angle Ru–N–O this was disregarded in the present calculation and C_{4v} symmetry maintained. Distances reported [15] for $[Ru(NH_3)_5NO]^{+3}$ were used, and are: Ru–NO = 1.80 Å, Ru–NH_3(*cis*) = 2.09 Å, Ru–NH_3(*trans*) = 2.19 Å, N–O = 1.11 Å. The same approximation as above was made regarding the Ru–N–O angle. The distance Ru–NH_3 = 2.10 Å was assumed for the hexammine complexes (O_h symmetry).

The orbitals 4d, 5s and 5p of Ruthenium were included in the calculation. Wave functions for these orbitals were those given by Basch and Gray* [16]. For the CN ligands, the highest energy σ and π orbitals, as well as the lowest π^*, were included. Wave functions for these orbitals were those used in the Molecular Orbital calculation of the pentakis(cyano-C), nitrosylferrate(–2) complex ion [17], obtained by a Wolfsberg–Helmholz calculation of cyanide ion on a basis of Clementi's double-ζ [18] atomic functions for C and N**. Wave functions for NO highest energy σ and π, and lowest π^* orbitals used were those calculated by Brion, Moser and Yamasaki [19] based on Slater-type atomic orbitals. Wave functions used for Cl (3s and 3p) were Clementi's double-ζ*** [18]. For the ammine complexes, a further approximation was made, regarding the ligands NH_3: due to computational difficulties, only nitrogen orbitals (2s and 2p) were considered in the wave functions of these ligands. This approximation may be justified in part by considering the difference in electronegativity between N and H. Wave functions used for N were Clementi's doublet-ζ [18].

*For charge + 1, configuration ...$4d^7$ (4d) and ...$4d^5$ 5s 5p (5s and 5p).

**For neutral atoms, configurations ...$2s^2$ $2p^2$ (3P) for carbon, ...$2s^2$ $2p^3$ (4S) for nitrogen.

***For neutral atom, configuration ...$3s^2$ $3p^5$ (2P).

Symmetry orbitals for the calculation of group overlap integrals were obtained by standard methods. Overlap integrals were calculated exactly. VOIPS for Ruthenium were obtained from reference 20. Energies of the CN orbitals used were: σ = –112.0 kcm^{-1}, π = –122.0 kcm^{-1} and π^* = –30.0 kcm^{-1} [15]. Energies of the NO orbitals were: σ = –118.74 kcm^{-1}, π = –120.05 kcm^{-1} and π^* = –74.61 kcm^{-1} [17]. Energies used for Cl orbitals were: 3s = –203.8 kcm^{-1}, $3p_\sigma$ = –120.4 kcm^{-1} and $3p_\pi$ = –110.4 kcm^{-1} [7, 21]; for N orbitals of the NH_3 ligands, were used: 2s = –206.2 kcm^{-1}, $2p_\sigma$ = –116.4 kcm^{-1} and $2p_\pi$ = –106.4 kcm^{-1} [7, 21].

Self-consistency in charge and configuration was carried on up to 0.0005 in all cases. For some of the complexes studied negative populations were obtained for the 5p orbitals of Ruthenium. Such unphysical situation has been reported for other SCCC–MO calculations [22, 23], when Mulliken population analysis was used, and it may be circumvented by changing population definitions [23]. However we realize that any such definitions are necessarily arbitrary; since we were mainly interested in the 4d and 5s populations of Ru, and mainly in general trends, we have maintained Mulliken definitions.

Energy Levels

Tables I and II present the energy levels obtained for the ground state of the complex ions of O_h and C_{4v} symmetries, respectively. These tables also show the main contributions of orbitals involved in each level, in terms of their Mulliken populations. Among the octahedral complexes, $[Ru(CN)_6]^{-4}$ and $[Ru(NH_3)_6]^{+2}$ show a closed-shell structure, as expected, the last occupied orbital being of t_{2g} symmetry and localized mainly on the metal. $[Ru(NH_3)_6]^{+3}$ has an open-shell structure with 5 electrons on the last

TABLE I. Molecular Orbital Results for Octahedral Ruthenium Complexes.

$[Ru(CN)_6]^{-4}$			$[Ru(NH_3)_6]^{+2}$			$[Ru(NH_3)_6]^{+3}$		
Molecular orbital	Energy (Kcm^{-1})	Orbital populations[a]	Molecular orbital	Energy (Kcm^{-1})	Orbital populations[a]	Molecular orbital	Energy (Kcm^{-1})	Orbital populations[a]
$1a_{1g}$	- 149.65	80.5 σ(CN), 19.5(5s(Ru))	$1a_{1g}$	- 221.52	97.0(2s (N))	$1a_{1g}$	- 222.13	95.3(2s(N))
$1t_{2g}$	- 132.49	94.4 π(CN)	$1t_{1u}$	- 210.69	106(2s(N))	$1t_{1u}$	- 208.54	105(2s(N))
$1t_{1u}$	- 130.80	83.3 π(CN), 19.6 σ(CN)	$1e_g$	- 200.64	95.1(2s(N))	$1e_g$	- 201.87	93.7(2s(N))
$1t_{2u}$	- 118.31	100 π(CN)	$2a_{1g}$	- 129.50	91.1($2p_\sigma$(N))	$2a_{1g}$	- 130.39	90($2p_\sigma$(N))
$1e_g$	- 116.83	60.9 σ(CN), 39.1(4d(Ru))	$1t_{2g}$	- 123.60	63.2($2p_\pi$ (N)), 36.8(4d(Ru))	$2e_g$	- 127.24	58.8($2p_\sigma$(N)),39.9(4d(Ru))
$1t_{1g}$	- 111.44	99.8 π(CN)	$2e_g$	- 123.17	64.5($2p_\sigma$ (N)), 34.9(4d(Ru))	$1t_{2g}$	- 127.13	50.9($2p_\pi$(N)), 49.1(4d(Ru))
$2t_{1u}$	- 104.09	79.5 σ(CN), 18.3 π(CN)	$2t_{1u}$	- 119.29	75.4($2p_\sigma$ (N)),23.9($2p_\pi$ (N))	$2t_{1u}$	- 119.52	74.2($2p_\sigma$(N)), 23.3($2p_\pi$(N))
$2t_{2g}$[b]	- 75.74	92.1(4d(Ru))	$1t_{2u}$	- 104.12	100($2p_\pi$ (N))	$1t_{2u}$	- 104.12	100($2p_\pi$(N))
$2e_g$	- 42.03	60.9(4d(Ru)), 39.1 σ(CN)	$3t_{1u}$	- 102.52	75.4($2p_\pi$ (N)), 23.9($2p_\sigma$(N))	$3t_{1u}$	- 102.56	75.7($2p_\pi$(N)), 23.6($2p_\sigma$(N))
$3t_{1u}$	- 30.63	96.1 π^*(CN)	$1t_{1g}$	- 98.67	100($2p_\pi$ (N))	$1t_{1g}$	- 98.67	100($2p_\pi$(N))
$3t_{2g}$	- 28.83	98.0 π^*(CN)	$2t_{2g}$[c]	- 88.75	63.2(4d(Ru)), 36.8($2p_\pi$(N))	$2t_{2g}$[d]	- 92.13	50.9(4d(Ru)), 49.1($2p_\pi$(N))
$2t_{2u}$	- 28.02	100 π^*(CN)	$3e_g$	- 61.50	60.6(4d(Ru)), 35.1($2p_\sigma$(N))	$3e_g$	- 60.26	54.1(4d(Ru)), 40.9($2p_\sigma$(N))
$2t_{1g}$	- 24.15	99.8 π^*(CN)	$4t_{1u}$	34.80	106(5p(Ru))	$4t_{1u}$	45.33	104(5p(Ru))
$4t_{1u}$	16.28	96.9(5p(Ru))	$3a_{1g}$	81.96	91.9(5s(Ru))	$3a_{1g}$	103.34	89.2(5s(Ru))
$2a_{1g}$	46.06	80.5(5s(Ru), 19.5 σ(CN)						
Energy of metal orbitals[e]:			Energy of metal orbitals[e]			Energy of metal orbitals[e]		
4d: - 81.27			4d: - 104.79			4d: -111.89		
5s: - 63.91			5s: - 80.78			5s: - 84.51		
5p: - 23.31			5p: - 40.08			5p: - 43.60		
F - factors:			F - factors:			F - factors:		
F_σ (metal-ligand) = 2.3			F_σ (metal-ligand) = 1.77			F_σ (metal-ligand) = 1.83		
F_π (metal-ligand) = 2.0			F_π (metal-ligand) = 2.0			F_π (metal-ligand) = 2.0		
F (ligand-ligand) = 2.0			F (ligand-ligand) = 2.0			F (ligand-ligand) = 2.0		

a) In % of one electron; only orbitals contributing with 10% or more are included. b) Highest occupied orbital, with 6 electrons. c) Highest occupied orbital, with 6 electrons. d) Highest occupied orbital, with 5 electrons. e) After self-consistency.

TABLE II. Molecular Orbital Results for Ruthenium Complexes of C_{4v} Symmetry.

	$[Ru(CN)_5NO]^{-2}$ (a)		$[Ru(NH_3)_5NO]^{+3}$ (c)		$[RuCl_5NO]^{-2}$ (b)	
M.O.	Energy (Kcm^{-1})	Orbital Populations (d)	Energy (Kcm^{-1})	Orbital Populations (d)	Energy (Kcm^{-1})	Orbital Populations (d)
$1a_1$	- 149.89	63.2σ(CN),21.8(5s(Ru)),14.7σ(NO)	- 221.17	91.1(2s(N))	- 211.83	95.1(2s(Cl))
$1b_2$	- 139.30	78.9π(CN), 21.4(4d(Ru))	- 207.19	103(2s(N))	- 206.27	103(2s(Cl))
1e	- 138.27	65.4π(CN),23.0(4d(Ru)),10.6π(NO)	- 205.00	96.5(2s(N))	- 203.25	98.9(2s(Cl))
$2a_1$	- 132.63	36.0π(CN),33.7σ(NO),19.7(4d(Ru))	- 203.37	91.4(2s(N))	- 201.65	96.6(2s(Cl))
2e	- 129.00	58.3π(CN),19.4σ(CN),17.6π(NO)	- 136.57	45.4σ(NO),22.5(2p_σ(N)),21.9(4d(Ru))	- 139.26	69.7(2p_σ(Cl)),14.8σ(NO),11.3(5s(Ru))
$3a_1$	- 128.48	41.0π(CN),27.1(4d(Ru)),26.3σ(CN)	- 133.27	41.0(4d(Ru)),29.0π(NO),27.9(2p_π(N))	- 128.85	36.9(4d(Ru)),32.4σ(NO),29.4(2p_σ(Cl))
$1b_1$	- 124.28	52.9(4d(Ru)), 47.1σ(CN)	- 132.03	54.1(2p_π(N)), 45.9(4d(Ru))	- 125.98	63.2(2p_σ(Cl)), 36.5(4d(Ru))
3e	- 118.94	54.7π(CN), 45.0π(NO)	- 130.39	73.7(2p_σ(N)), 17.7(4d(Ru))	- 125.70	45.5(2p_σ(Cl)),37.9π(NO),13.1(2p_π(Cl))
$2b_1$	- 118.31	100π(CN)	- 128.71	62.8(2p_σ(N)), 35.0(4d(Ru))	- 124.04	48.8(2p_π(Cl)),19.3(2p_σ(Cl)),17.5π(NO),
4e	- 113.42	82.1π(CN), 16.7π(NO)	- 121.06	54.8(2p_σ(N)),22.9(2p_π(N)),15.1σ(NO)		14.4(4d(Ru))
$1a_2$	- 111.44	99.8π(CN)	- 120.84	57.0(2p_σ(N)), 22.1(2p_π(N)),14.4π(NO)	- 123.63	49.7(2p_σ(Cl)),31.5(2p_π(Cl)),17.9σ(NO)
$4a_1$	- 106.84	50.0σ(CN),21.9π(CN),24.1σ(NO)	- 113.74	51.4π(NO),22.2(2p_π(N)),20.1(2p_σ(N))	- 122.86	80.2(2p_π(Cl)), 19.8(4d(Ru))
5e	- 104.51	73.5σ(CN), 20.0π(CN)	- 104.06	100(2p_π(N))	- 114.23	45.1(2p_π(Cl)),39.7π(NO)),10.9(2p_σ(Cl))
6e	- 91.09	50.5(4d(Ru)),24.8π^*(NO),16.7π(CN)	- 103.91	72.8(2p_π(N)),14.8(2p_σ(N)),12.0σ(NO)	- 107.61	100(2p_π(Cl))
$2b_2$(e)	- 86.29	75.3(4d(Ru)), 20.9π(CN)	- 103.16	86.2(2p_π(N)), 12.8(2p_σ(N))	- 106.70	68.0(2p_π(Cl)),17.3(2p_σ(Cl)),13.4σ(NO)
7e	- 64.80	70.0 π^*(NO), 21.8(4d(Ru))	- 101.29	91.8(2p_π(N))	- 106.24	80.1(2p_π(Cl)), 17.5(2p_σ(Cl))
$3b_1$	- 54.58	52.9σ(CN), 47.1(4d(Ru))	- 98.47	100(2p_π(N))	- 102.46	92.0(2p_π(Cl))
$5a_1$	- 48.51	49.4(4d(Ru)),32.7σ(CN),16.2σ(NO)	- 88.34	44.2(2p_π(N)),33.3(4d(Ru)),19.9 π^*(NO)	- 100.35	100(2p_π(Cl))
$6a_1$	- 33.61	86.4 π^*(CN), 12.2(5p(Ru))	- 82.14	54.1(4d(Ru)), 45.9(2p_π(N))	- 96.05	71.1(4d(Ru)), 20.9(2p_π(Cl))
8e	- 32.08	87.4 π^*(CN), 11.0(5p(Ru))	- 66.41	75.1(π^*(NO)),18.6(4d(Ru))	- 95.56	80.2(4d(Ru)), 19.8(2p_π(Cl))
$4b_1$	- 28.02	100 π^*(CN)	- 53.47	54.3(4d(Ru)),21.6σ(NO),20.9(2p_σ(N))	- 71.15	92.7 π^*(NO)
9e	- 26.87	97.3 π^*(CN)	- 47.81	56.5(4d(Ru)), 37.1(2p_σ(Cl))	- 63.41	60.5(4d(Ru)), 36.5(2p_σ(Cl))
$3b_2$	- 26.13	96.5 π^*(CN)	30.86	91.4(5p(Ru))	- 60.16	58.9(4d(Ru)),20.5(2p_σ(Cl)),18.6σ(NO)
10e	- 25.20	98.5 π^*(CN)	74.62	98.2(5p(Ru))	12.13	96.4(5p(Ru))
$2a_2$	- 24.15	99.8 π^*(CN)	127.33	79.9(5s(Ru)), 10.4(2p_σ(N))	32.63	104(5p(Ru))
11e	25.49	82.3(5p(Ru)), 12.7 π^*(CN)			80.37	81.2(5s(Ru)), 10.8(2p_σ(Cl))
$7a_1$	26.27	67.5(5s(Ru)),18.0σ(CN),11.1(5p(Ru))				
$8a_1$	36.75	70.6(5p(Ru)),10.3(5s(Ru)),11.6 π^*(CN)				

a) For F_σ (metal–ligand) = 2.1, F_π (metal–ligand) = 2.4, F(ligand–ligand) = 2.0. Energies of metal orbitals after self-consistency: 4d = –100.37, 5s = –75.66, 5p = –34.94 k cm^{-1}.
b) For F_σ (metal–ligand) = 1.9, F_π (metal–ligand) = 1.8, F(ligand–ligand) = 2.0. Energies of metal orbitals after self-consistency: 4d = –102.54; 5s = –78.13, 5p = –37.12 k cm^{-1}.
c) For F_σ (metal–ligand) = 2.0, F_π (metal–ligand) = 2.4, F(ligand–ligand) = 2.0. Energies of metal orbitals after self-consistency: 4d = –109.18, 5s = –81.66, 5p = –40.87 k cm^{-1}.
d) In % of one electron; only orbitals contributing with 10% or more are included. e) Highest occupied orbital, with 2 electrons.

TABLE III. Electronic Transitions of $|Fe(CN)_6|^{-4}$ and $|Ru(CN)_6|^{-4}$.

$\|Fe(CN)_6\|^{-4}$			$\|Ru(CN)_6\|^{-4}$		
Experimental[a]		Calculated[b]	Experimental[a]		Calculated[c]
$\nu_{max}(kcm^{-1})$	$f \times 10^2$	$\nu(kcm^{-1})$	$\nu_{max}(kcm^{-1})$	$f \times 10^2$	$\nu(kcm^{-1})$
23.7	0.002		31.0 } $\Delta = 33.8$	–	$33.7(2t_{2g} \rightarrow 2e_g)$
31.0 } $\Delta = 33.8$	0.84	$34.5(2t_{2g} \rightarrow 3e_g)$			
37.0	0.47				
45.9	53.5	$46.9(2t_{2g} \rightarrow 4t_{1u})$	48.5	85	$45.1(2t_{2g} \rightarrow 3t_{1u})$
50.0	2.3	$53.0(2t_{2g} \rightarrow 2t_{2u})$	52.0	45	$47.7(2t_{2g} \rightarrow 2t_{2u})$
$\|E(3d) - E(2t_{2g})\| = 16.32$			$\|E(4d) - E(2t_{2g})\| = 5.27$		
$\|E(3d) - E(3e_g)\| = 50.86$			$\|E(4d) - E(2e_g)\| = 39.27$		

[a]From references 21, 22 and 23, in aqueous solution. [b]From reference 21. [c]This work.

occupied orbital (metal t_{2g}). In all three cases, the lowest energy empty orbital is e_g (metal).

Complexes of C_{4v} symmetry are all of closed shell structure. In this symmetry the last occupied and first empty t_{2g} and e_g orbitals are split into b_2, e and a_1, b_1 respectively. The ordering of the level energies in the three cases is $e < b_2 < b_1 < a_1$, except for $[Ru(NH_3)_5NO]^{+3}$ where the ordering $a_1 < b_1$ is obtained. This inversion may be explained by the greater *trans* $Ru-NH_3$ distance, relative to the *cis*, used for this last complex.

All three complex ions of C_{4v} symmetry show a level whose main contribution is from the π^* (NO) orbital, between the highest occupied and lowest empty d levels. The positioning of this level between the metal d levels persists for several values of the parameter F around 2.0.

Electronic Spectrum of $[Ru(CN)_6]^{-4}$

The electronic spectrum in aqueous solution of $[Ru(CN)_6]^{-4}$ shows a small number of bands [24, 25], as would be expected of a low-spin d^6 configuration. From the $^1A_{1g}$ ground state only transitions to $^1T_{1u}$ states are allowed. Those may correspond to charge transfer transitions of metal → ligand type ($t_{2g} \rightarrow t_{1u}$, $t_{2g} \rightarrow t_{2u}$) or ligand → metal ($t_{2u} \rightarrow e_g$, $t_{1u} \rightarrow e_g$). Gray *et al.* [24, 25] assigned the high-intensity bands to metal → ligand type transitions, that is transitions from the highest t_{2g} (metal) orbital to the empty t_{1u} and t_{2u} orbitals localized mainly on the π^* (CN) orbital. Our M.O. calculation supports this assignment, since ligand → metal transitions would occur at considerably higher energies.

Table III shows experimental and calculated transitions for $[Ru(CN)_6]^{-4}$. The energy difference between the t_{2g} and e_g levels was fitted to the value of Δ [24, 25]. The same table shows also data on the electronic spectra in solution of $[Fe(CN)_6]^{-4}$ and its assignment made by Alexander and Gray [23, 25] based on an M.O. calculation with the same method. These authors suggested that the remarkably small increase of Δ that occurs for cyanides of the Fe family (Fe, Ru, Os) is due to compensation between two effects. One is the stabilization of the highest occupied t_{2g} level due to stronger $d-\pi^*$ (CN) bonding. If this effect is stronger in the order Ru > Fe, the t_{2g} level is stabilized to a greater extent in the Ru complex. On the other hand, since Δ values are equivalent, one expects a compensation of this effect produced by a weaker σ interaction of the d orbitals in $[Ru(CN)_6]^{-4}$ respect to $[Fe(CN)_6]^{-4}$, due to the increased number of nodes in the Ru orbitals, lowering the energy of the e_g orbital in the first complex.

In Table III it is seen that our calculation supports this hypothesis. In this table are given the energies of the t_{2g} and e_g orbitals involved relative to the energies of the 3d and 4d orbitals in the complexes of Fe and Ru.

Populations obtained for the π^*(CN) orbital also suggest that Ru is a better back-donor than Fe with respect to CN: these are 0.07 for $[Fe(CN)_6]^{-4}$ and 0.133 for $[Ru(CN)_6]^{-4}$.

Electronic Spectra of $[Ru(NH_3)_6]^{+2}$ and $[Ru(NH_3)_6]^{+3}$

The electronic spectra in solution of $[Ru(NH_3)_6]^{+2}$ was measured by other authors [26–30] who report a peak at 25–26 kcm^{-1} with $\epsilon_{max} = 30$–40, another at around 36 kcm^{-1} with $\epsilon_{max} \sim 650$ and a band of high intensity at energies greater than 45 kcm^{-1}.

The interpretation of this spectrum is not yet clear. Although at first glance the low-energy bands could be assigned to the d → d transitions $^1A_{1g} \rightarrow$

TABLE IV Electronic Spectrum of $[Ru(NH_3)_6]^{+3}$

Experimental[a]				Calculated[b]	
ν_{max} (kcm^{-1})	$\Delta\nu_{1/2}$ (kcm^{-1})	ϵ_{max}	f × 10^2	ν (kcm^{-1})	
23 0	~4	0 5	0 8 × 10^{-3}	23 0	(d → d) ($^2T_{2g} \rightarrow {}^4T_{1g}$)
30 9	4 4	70	0 13	29 0 29 4 31 7	(d → d) ($^2T_{2g} \rightarrow {}^2T_{1g}$) ($^2T_{2g} \rightarrow {}^2A_{2g}$) ($^2T_{2g} \rightarrow {}^2T_{2g}$)
35 6	3 7	260	0 41	34 0 36 3 36 3	($^2T_{2g} \rightarrow {}^2E_g$) (d → d) ($^2T_{2g} \rightarrow {}^2T_{1g}$) ($^2T_{2g} \rightarrow {}^2T_{2g}$)
38 5	5 4	330	0 77	38 6 38 4	(d → d) ($^2T_{2g} \rightarrow {}^2A_{1g}$) I → M charge transfer ($^1t_{1g} \rightarrow {}^3e_g$)
47 6	7 2	470	1 42	43 7	(d → d) ($^2T_{2g} \rightarrow {}^2E_g$)
>50	–	very high	very high	42 0	I → M charge transfer ($^3t_{1u} \rightarrow 3e_g$)

[a] After Gaussian decomposition [b] See text

$^1T_{1g}$ and $^1A_{1g} \rightarrow {}^1T_{2g}$, Schmidtke and Garthoff [26] have shown that the band around 36 kcm^{-1} cannot be assigned to the second d → d transition, since this would lead to an unreal value of the Racah parameter B Based on spectra of other ammine d^6 complexes of Ru, these authors have proposed a value for Δ = 27 1 kcm^{-1} for this complex to which we have fitted the $t_{2g} \rightarrow e_g$ transition in our M O calculation

We have measured the spectrum of $[Ru(NH_3)_6]^{+2}$ in aqueous solution of NH_3 and N_2 atmosphere, in an attempt to delay decomposition of this highly unstable complex We verified that the spectrum changes rapidly with time In fact, when the spectrum is taken less than 2 minutes after dissolution, two low-energy bands are obtained, one at 25 kcm^{-1} with ϵ_{max} = 225 and another at 36 4 kcm^{-1} with ϵ_{max} = 545 Ten minutes after dissolution, the same bands show ϵ_{max} = 40 and $\epsilon_{max} \cong 700$, respectively, which are approximately the values reported by the other authors Figure 1 shows the spectrum taken immediately after dissolution

As for the transition at 36 4 kcm^{-1}, we suggest assigning it to the ligand (π) → metal (4d) charge transfer $1\,t_{1g} \rightarrow 3e_g$, which our molecular orbital calculation predicts to occur at ≅37 kcm^{-1} Low intensity could be due to the parity-forbidden nature of the transition This band could be obscuring the peak due to the d → d transition $^1A_{1g} \rightarrow {}^1T_{2g}$, whose maximum would occur at slightly lower energy It is difficult to explain the increase with time of the intensity of this band, since the decomposition products are not known However, $[Ru(NH_3)_6]^{+3}$ may be formed and it does show bands in this region, as shall be seen

Two bands in the low-energy region have been reported for $[Ru(NH_3)_6]^{+3}$, namely at ν_{max} = 31 3 kcm^{-1} ($\epsilon_{max} \cong 100$) and ν_{max} = 36 4 kcm^{-1} (ϵ_{max} = 480) [29, 30] We have measured again the spectrum of this complex in aqueous solution, which is presented in Fig 2 As expected of a d^5 configuration, this spectrum shows a complex structure Many d → d transitions may be expected from the $^2T_{2g}$ ground state, the interpretation is also rendered difficult by the possibility of low-energy charge transfer transitions of the ligand → metal type, to the highest occupied t_{2g} level We shall not attempt to give here a definite interpretation of this spectrum, rather we shall suggest a value of Δ which we believe is consistent with its characteristics

First we notice the band at 23 kcm^{-1} with ϵ_{max} = 0 5 Such low intensity allows one to assign it to the first spin-forbidden d → d transition, namely $^2T_{2g} \rightarrow {}^4T_{1g}$ Through the diagonal elements of the energy matrix [31] for octahedral d^5, a value of Δ = 32 7 kcm^{-1} is obtained if we assume B = 0 46 kcm^{-1} and C/B = 4 This value of B is consistent with the value 0 43 kcm^{-1} derived for various hexamines of d^6 configuration [25], since the nephelauxetic effect of charge increase would be to slightly increase B The increase in Δ from $[Ru(NH_3)_6]^{+2}$ to $[Ru(NH_3)_6]^{+3}$ is of the same order as that observed for Fe complexes of the same charges with the similar ligand H_2O [24]

With these values of Δ and B, other d → d transitions were calculated in the same manner As is shown in Table IV, calculated energies (for the excited configuration $t_{2g}^4\,e_g^1$) fall in the same region as the observed transitions, supporting the suggested value of Δ

We now turn to charge-transfer type transitions Our results for the M O energy levels (after approximately fitting the $t_{2g} \rightarrow c_g$ energy difference to the value of Δ given above) show a number of levels quite near in energy to the highest filled t_{2g} from which

TABLE V. Electronic Spectrum of $[Ru(CN)_5NO]^{-2}$

Experimental[a]		Calculated	
$\nu_{max}(kcm^{-1})$	ϵ_{max}	ν (kcm^{-1})	
22.2	650	21.5	$^1A_1 \rightarrow {}^1E$ ($2b_2 \rightarrow 7e$)
26.8	200	26.3	$^1A_1 \rightarrow {}^1A_1$ ($6e \rightarrow 7e$)
32.0	300	30.2[b]	$^1A_1 \rightarrow {}^1A_2$ ($2b_2 \rightarrow 3b_1$)
37.5	1000	38.0[b]	$^1A_1 \rightarrow {}^1E$ ($6e \rightarrow 3b_1$)
43.5	9000	44.0[b]	$^1A_1 \rightarrow {}^1E$ ($6e \rightarrow 5a_1$)
52.0	20000	54.2	$^1A_1 \rightarrow {}^1E$ ($2b_2 \rightarrow 8e$)

[a]After Gaussian decomposition of the spectrum. [b]Corrected for interelectronic repulsion, assuming B = 400 cm^{-1} and C/B = 4.63.

transitions to this last level could occur, contributing to the series of bands seen in the low-energy region. However, the present data is not sufficient to make unambiguous assignments. Other experimental results (mainly low-temperature measurements) would be necessary.

In Table IV we have pointed out that the band at 38.5 kcm^{-1} could also be due to the ligand → metal charge transfer $1t_{1g} \rightarrow 3e_g$, if this same transition does occur in $[Ru(NH_3)_6]^{+2}$. The good agreement between calculated and observed energies in both complexes supports this assignment.

As to the high intensity band with $\nu_{max} > 50$ kcm^{-1}, it must be due to charge transfer transition(s) to the first empty e_g level, both symmetry and parity allowed. Our calculation predicts the first of these transitions ($3t_{1u} \rightarrow 3e_g$) to occur at 42 kcm^{-1}.

Electronic Spectra of $[Ru(CN)_5NO]^{-2}$, $[RuCl_5NO]^{-2}$ and $[Ru(NH_3)_5NO]^{+3}$

Optical spectra of these complex ions have been measured by us in solution [8] (Figures 3, 4 and 5).

For these complexes, only transitions of the type $^1A_1 \rightarrow {}^1A_1$ and $^1A_1 \rightarrow {}^1E$ are allowed. In all three cases, the presence of the e level corresponding to an orbital mainly of π^* (NO) character as the lowest-energy empty level leads to assigning the lowest-energy bands to charge-transfer transitions from the highest occupied metal d levels e and b_2 to e (π^*-(NO)).

The spectra of $[Ru(CN)_5NO]^{-2}$ is very similar [17] to that of $[Fe(CN)_5NO]^{-2}$ which has led us to adopt the same interpretation (in the case of the pentacyanoferrate(II) complex, the assignments were supported by measurements made at low temperature and with polarized light). Calculated and experimental transition energies are in very good agreement, as seen in Table V. d → d transitions were corrected for interelectronic repulsions. The high-energy band ($\nu_{max} > 50$ kcm^{-1}) was assigned to a charge transfer transition of the type metal → ligand (π^*(CN)).

Tables VI and VII present the electronic transitions both measured and calculated of $[RuCl_5NO]^{-2}$ and $[Ru(NH_3)_5NO]^{+3}$, respectively. Agreement between theoretical and experimental values for the lower energy transitions is not so good as in the case of the pentacyanoruthenate(II) complex, so that assignments should be regarded as tentative. High-energy charge-transfer transitions in $[RuCl_5NO]^{-2}$ and $[Ru(NH_3)_5NO]^{+3}$ have been assigned to ligand → metal type transitions. The specific assignments made for transitions of this type were based on good agreement between calculated and experimental values.

It should be noticed that the bands assigned to 4d → π^*(NO) charge transfer transitions are of low intensity, which is unexpected since these are symmetry allowed. This could be due to the fact that the lowest-energy empty e(π^*(NO)) orbital has also some contribution from the 4d orbital of Ruthenium. This point could be clarified by calculations of the oscillator strengths of the mentioned transitions, but better wave functions than those obtained by a semi-empirical method would probably be required.

TABLE VI. Electronic Spectrum of $[Ru\,Cl_5\,NO]^{-2}$.

Experimental[a]				Calculated	
$\nu_{max}(kcm^{-1})$	ϵ_{max}	$\Delta\nu_{1/2}(kcm^{-1})$	$f \times 10^2$	ν (kcm^{-1})	
17.6	17	2.9	0.021	24.4	$^1A_1 \rightarrow {}^1E$ ($2b_2 \rightarrow 8e$)
19.6	60	3.7	0.096	24.9	$^1A_1 \rightarrow {}^1A_1$ ($7e \rightarrow 8e$)
27.7	112	6.7	0.32	30.4[b]	$^1A_1 \rightarrow {}^1A_2$ ($2b_2 \rightarrow 4b_1$)
32.1	950	4.4	1.8	32.9[b]	$^1A_1 \rightarrow {}^1E$ ($7e \rightarrow 4b_1$)
39.5	9800	7.0	30	39.3[b]	$^1A_1 \rightarrow {}^1E$ ($7e \rightarrow 7a_1$)
				39.0[c]	$^1A_1 \rightarrow {}^1E$ ($6e \rightarrow 4b_1$)
47.1	31000	5.1	68	46.1[c]	$^1A_1 \rightarrow {}^1E$ ($5e \rightarrow 7a_1$)
>52.0	very high	–	very high	50.8[c]	$^1A_1 \rightarrow {}^1E$ ($4e \rightarrow 4b_1$)

[a]After Gaussian decomposition of the spectrum. [b]Corrected for interelectronic repulsion, assuming B = 400 cm^{-1} and C/B = 4.63. [c]Ligand → metal charge transfer.

TABLE VII. Electronic Spectrum of $[Ru(NH_3)_5NO]^{+3}$.

Experimental[a]				Calculated
$\nu_{max}(kcm^{-1})$	ϵ_{max}	$\Delta\nu_{1/2}(kcm^{-1})$	$f \times 10^2$	$\nu(kcm^{-1})$
21.1	10	3.9	0.017	15.7 $^1A_1 \rightarrow {}^1E$ $(2b_2 \rightarrow 8e)$
24.0	8	4.3	0.015	21.9 $^1A_1 \rightarrow {}^1A_1$ $(7e \rightarrow 8e)$
30.4	26	4.8	0.054	32.2[b] $^1A_1 \rightarrow {}^1A_2$ $(2b_2 \rightarrow 4b_1)$
33.2	45	3.5	0.068	33.7[b] $^1A_1 \rightarrow {}^1E$ $(7e \rightarrow 7a_1)$
48.0	2300	7.9	8	46.0[b] $^1A_1 \rightarrow {}^1E$ $(7e \rightarrow 4b_1)$
				47.8[c] $^1A_1 \rightarrow {}^1E$ $(6e \rightarrow 7a_1)$
>52.0	very high		very high	53.5[c] $^1A_1 \rightarrow {}^1E$ $(6e \rightarrow 4b_1)$

[a]After Gaussian decomposition of the spectrum. [b]Corrected for interclectronic repulsion, assuming B = 400 cm^{-1} and C/B = 4.63. [c]Ligand → metal charge transfer.

TABLE VIII. Isomer Shifts and Electron Populations of Ruthenium Complexes.

Complex	Isomer Shift[a] (mm/s)	Populations			
		4d	5s	π^*(CN)	π^*(NO)
$[Ru(NH_3)_6]I_2$	-0.93 ± 0.03[c]				
$[Ru(NH_3)_6]Cl_2$	-0.92 ± 0.01[c]	7.595	0.142		
$[Ru(NH_3)_6](BF_4)_2$	-0.92 ± 0.01[c]				
$[Ru(NH_3)_6]Br_3$	-0.50 ± 0.06[c]	7.300	0.234		
$[Ru(NH_3)_6]Cl_3$	-0.49 ± 0.01[b]				
$K_4[Ru(CN)_6]$	-0.22 ± 0.01[b]	7.440	0.391	0.133	
	-0.25 ± 0.03[d]				
$K_2[RuCl_5NO]$	-0.36 ± 0.03[c]	7.356	0.307		0.294
$Rb_2[RuCl_5NO]$	-0.37 ± 0.03[e]				
$[Ru(NH_3)_5NO]Cl_3 \cdot H_2O$	-0.19 ± 0.01[c]	7.028	0.360		0.961
	-0.20 ± 0.03[e]				
$[Ru(NH_3)_5NO]Br_3 \cdot H_2O$	-0.22 ± 0.02[c]				
$[Ru(NH_3)_5NO]SO_4(S_2O_8)_{1/2}$	-0.20 ± 0.01[c]				
$K_2[Ru(CN)_5NO] \cdot 2H_2O$	-0.08 ± 0.01[c]	6.975	0.440	0.126	1.112
	$+0.03 \pm 0.03$[d]				
$K_2[Ru(CN)_5NO]$	-0.12 ± 0.03[e]				

[a]Isomer shifts of the recoilless 90 keV γ rays of ^{99}Ru, relative to Ru metal. [b]G. Kaindl, W. Potzel, F. E. Wagner, U. Zahn and R. L. Mössbauer, *Z. Phys., 226,* 103 (1969). [c]W. Potzel, F. E. Wagner, U. Zahn, R. L. Mössbauer and J. Danon, *Z. Phys., 240,* 306 (1970). [d]C. A. Clausen, R. A. Prados and M. L. Good, *J. Am. Chem. Soc., 92,* 7482 (1970). [e]R. Greatrex, N. N. Greenwood and P. Kaspi, *J. Chem. Soc. A,* 1873 (1971).

Mössbauer Hyperfine Interactions

Recoilless resonance may be obtained with the 90 keV γ rays of ^{99}Ru. In spite of the relatively small number of reports on Mössbauer measurements for this element up to date, a significant amount of data is already available on hyperfine parameters in Ru complexes, namely isomer shifts and quadrupole interactions [4–6].

The isomer shift (δ) is a consequence of the electrostatic monopole interaction between the electronic charge of an atom and the charge distribution inside its nucleus. The δ of an absorber relative to a source is given by

$$\delta = \frac{2\pi Ze^2}{5}(\langle R^2\rangle_{e.s.} - \langle R^2\rangle_{g.s.}) \times$$

$$\times [(\phi(0))^2_A - (\phi(0))^2_S] \qquad (1)$$

where Z is the atomic number of the nucleus, e the charge of the proton, $\langle R^2\rangle_{e.s.}$ and $\langle R^2\rangle_{g.s.}$ are the mean square radii of the nucleus at the excited and ground states respectively and $(\phi(0))^2_A$ and $(\phi(0))^2_S$ the electronic charge density at the nucleus for the

absorber and source, respectively. For Ru, the factor $(\langle R^2\rangle_{e.s.} - \langle R^2\rangle_{g.s.})$ is positive.

Differences in isomer shifts between different complexes of the same atom may be interpreted through a knowledge of the characteristics of the metal–ligand chemical bonds, which influence the atomic density at the nucleus. Electronic density at the nucleus (s electrons in the non-relativistic approximation) of a Mössbauer atom may be increased by bonding to ligands that are good σ-donors. On the other hand, ligands that have low-energy π^* orbitals available may be π-acceptors; in this case they may decrease the d population by receiving electronic density from the d_{xy}, d_{xz}, d_{yz} orbitals. Since d orbitals shield the nucleus from s electrons, this last effect also produces an increase in δ and has been observed in all Mössbauer spectra of transition metal complexes containing ligands such as CN, NO, *etc.* [3].

Table VIII shows values of δ measured for the Ru complexes studied. These values are compared to the 5s and 4d populations of Ru obtained through our M.O. calculations; populations of π-acceptor orbitals, namely π^*(NO) and π^*(CN), when present, are also included.

The lowest value of δ belongs to $[Ru(NH_3)_6]^{+2}$; in fact, this complex shows the smallest value for the 5s population, and highest value for 4d. Comparison with $[Ru(NH_3)_6]^{+3}$ shows the effect of increasing the charge: the δ value increases through loss of 4d electron density and increase of 5s population, this latter being due to greater σ invasion through a charge-compensation effect.

Comparison of the two octahedral complexes of Ru with formal configuration d^6, namely $[Ru(NH_3)_6]^{+2}$ and $[Ru(CN)_6]^{-4}$, shows clearly the effect of back-donation of the ligand CN, decreasing the d population in the latter complex. Also, 5s population is greater in the latter complex. The result of these effects is a higher value of δ for $[Ru(CN)_6]^{-4}$.

The influence of back-donation in δ values is seen very clearly for the three complexes containing the ligand NO. In particular, $[Ru(CN)_5NO]^{-2}$ shows the highest value of δ of this series of complexes. Comparison between this complex and the hexacyanoruthenate(II) complex, which exhibits a lower value of δ evidences the stronger back-donation effect of NO relative to CN, through the comparison of 4d populations and also of π^*(NO) and π^*(CN) populations. In the same way, comparison of the ammine complexes with and without the ligand NO evidences the role played by back-donation to this ligand.

The three complexes containing NO show differences in their δ values, which may be ascribed to the effect of the other ligands. Taking into account the approximations used regarding the ligands wave functions, the differences in 4d and π^*(NO) populations suggest that back donation to NO is different in the three complexes; also 5s(Ru) populations are in the order $CN > NH_3 > Cl$.

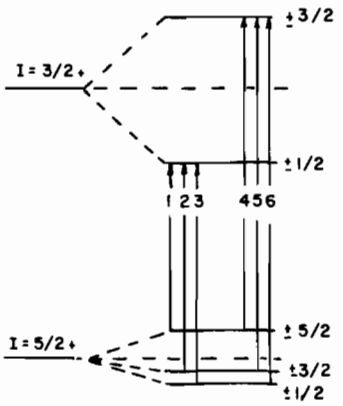

Figure 6. Quadrupole hyperfine levels in the $3/2^+ \rightarrow 5/2^+$ Mössbauer transition of ^{99}Ru.

Quadrupole splittings obtained in Mössbauer spectra are the consequence of the interaction of non-cubic extranuclear electric fields with the nuclear charge density, for nucleus with spin $I > 1/2$, in which case the nucleus has a quadrupole moment $Q \neq 0$. In Ru, the spin of the nucleus in the excited and ground states involved in the Mössbauer transition is 3/2 and 5/2, respectively.

Figure 6 shows the splitting of the nuclear energy levels of ^{99}Ru caused by quadrupole interaction. Experimentally, transitions 1, 2, 3 and 4, 5, 6 cannot be resolved between themselves [6]. In this case, the Mössbauer spectrum of ^{99}Ru under conditions leading to quadrupole splitting shows only 2 peaks, corresponding to the two groups of transitions.

The quadrupole splitting ΔE_Q of ^{99}Ru may be expressed as

$$\Delta E_Q = \frac{1}{2} e^2 \, qQ_{3/2} \, (1 + \eta^2/3)^{1/2} (1 - R) \qquad (2)$$

where $Q_{3/2}$ is the quadrupole moment of the nucleus in the excited state; $eq = -V_{zz}$ = the Z component of the electric field gradient tensor, e = the proton charge and η the assymmetry parameter ($\eta = (V_{xx} - V_{yy})/V_{zz}$), which is zero for C_{4v} symmetry; $(1 - R)$ is the Sternheimer factor.

In covalent complexes such as those studied here, the electric field gradient is believed to be almost entirely due to the non-cubic electronic charge distribution around the Mössbauer nucleus [32]. In this case, for complexes of C_{4v} symmetry q may be expressed as

$$q = \frac{4}{7} \langle r^{-3}\rangle_d \, [(n_{d_{x^2-y^2}} - n_{d_{z^2}}) + (n_{d_{xy}} - n_{d_{xz,yz}})] \qquad (3)$$

where $\langle r^{-3}\rangle_d$ is calculated with the d radial functions and $n_{d_{x^2-y^2}}$, *etc.*, are the populations of the

TABLE IX. Electric Quadrupole Splittings (ΔE_Q) of Ruthenium and Iron Complexes.

Complex	Experimental ΔE_Q(mm/s)	Populations d_{z^2}	$d_{x^2-y^2}$	d_{xy}	$d_{xz,yz}$	$(nd_{x^2-y^2} - nd_{z^2}) + (nd_{xy} - nd_{xz,yz})$	Calculated ΔE_Q (mm/s)
$K_2[RuCl_5NO]$	0.18 ± 0.02[a]	0.820	0.791	2.000	1.873	0.098	0.120
$[Ru(NH_3)_5NO]Cl_3 \cdot H_2O$	0.39 ± 0.01[a]						
	0.36 ± 0.03[c]						
$[Ru(NH_3)_5NO]Br_3 \cdot H_2O$	0.37 ± 0.02[a]	0.375[e]	0.904	0.870	2.000	1.627	0.339	0.353
$[Ru(NH_3)_5NO]SO_4(S_2O_8)_{1/2}$	0.38 ± 0.01[a]						
$K_2[Ru(CN)_5NO] \cdot 2H_2O$	0.39 ± 0.01[a]						
	0.49 ± 0.03[b]	0.427[e]	0.989	1.059	1.934	1.497	0.507	0.414
$K_2[Ru(CN)_5NO]$	0.40 ± 0.03[c]						
$K_2[Fe(CN)_5NO]$	1.726 ± 0.002[d]	0.954	1.019	1.977	1.517	0.525	1.788

[a]W. Potzel, F. E. Wagner, U. Zahn, R. L. Mössbauer and J. Danon, *Z. Phys., 240,* 306 (1970). [b]C. A. Clause, R. A. Prados and M. L. Good, *J. Am. Chem. Soc., 92,* 7482 (1970). [c]R. Greatrex, N. N. Greenwood and P. Kaspi, *J. Chem. Soc. A,* 1873 [d]J. Danon and L. Iannarella, *J. Chem. Phys., 47,* 382 (1967). [e]Average values.

different d orbitals. In expression (3) contributions due to p orbitals were considered negligible [32].

Table IX presents the values of the experimental quadrupole splittings of the complexes of C_{4v} symmetry studied here, as well as values of the calculated populations in the different d orbitals, and the factor in brackets in Eq. (3).

It is suggested from this table that differences in the quadrupole splittings in these complexes may be mainly a consequence of differences in back-donation to the ligand NO. In fact, this effect causes a decrease in the populations of the orbitals d_{xz}, d_{yz} relative to d_{xy} and is in the order $[Ru(CN)_5NO]^{-2} > [Ru(NH_3)_5NO]^{+3} > [RuCl_5NO]^{-2}$.

Quantitative results for the quadrupole splittings using the populations in Table IX may be obtained. Considering that $\langle r^{-3}\rangle_d$ must be smaller for d_{z^2}, $d_{x^2-y^2}$ than for d_{xy}, d_{xz}, d_{yz}, since the former are much more delocalized towards the ligands, we have made the approximation of neglecting the factor $(n_{d_{x^2-y^2}} - n_{d_{z^2}})$ in eq. (3).

Using the values $Q_{3/2}(^{99}Ru) = 0.29$ barn (estimated through an empirical rule) [33], $\langle r^{-3}\rangle_{4d} = 5.19$ a_0^{-3} (from Hartree–Fock calculations [34]), $(1 - R) = 0.68$ (the value generally accepted for Fe) [35], we have obtained the values of ΔE_Q given in Table IX.

Assuming a positive sign for $Q_{3/2}(^{99}Ru)$, which seems to be established [33, 36], it must be noticed that our calculations predict positive signs for ΔE_Q for all three C_{4v} complexes.

To further test the approximations used, we have calculated ΔE_Q for a complex containing a different Mössbauer element, namely $[Fe(CN)_5NO]^{-2}$. For this purpose we have repeated the SCCC–MO calculation for this complex ion, as performed in reference 17. After convergence to the same eigenvalues, eigenfunctions and total populations as in the original work, we obtained the populations given in Table IX. With these values we calculated ΔE_Q for this complex (Table IX), assuming $\langle r^{-3}\rangle_{3d} = 4.93$ a_0^{-3} (from reference 34) and $Q_{3/2}(^{57}Fe) = 0.2$ barn [35].

Considering the approximations used in calculating the 4d populations, the agreement between theoretical and experimental ΔE_Q values may be considered fair. These results support the assumption that distortions of d shells due to back-donation provide indeed the major contribution to the electric field gradient in complexes of Fe and Ru.

Acknowledgments

This work has been supported by the Conselho Nacional de Pesquisas. We are indebted to Drs. U. Wagner, F. Wagner, W. Potzel, L. Tosi and Professor J. P. Mathieu for valuable discussions.

References

1 W. P. Griffith, "The Chemistry of the Rarer Platinum Metals", Interscience, London (1967); F. A. Cotton and G. Wilkinson, "Advanced Inorganic Chemistry", Interscience, New York (1966).
2 C. J. Ballhausen and H. B. Gray, *Inorg. Chem., 2,* 426 (1963).
3 J. Danon, "Lectures on the Mössbauer Effect", Gordon and Breach, New York (1969); J. Danon, in "Mössbauer Spectroscopy and Its Applications", IAEA, Vienna (1972), p. 281.
4 G. Kaindl, W. Potzel, F. Wagner, U. Zahn and R. L. Mössbauer, *Z. Phys., 226,* 103 (1969); W. Potzel, F. E. Wagner, U. Zahn, R. L. Mössbauer and J. Danon, *Z. Phys., 240,* 306 (1970).

5 C. A. Clausen, R. A. Prados and M. L. Good, *J. Am. Chem. Soc., 92,* 7482 (1970).
6 R. Greatrex, N. N. Greenwood and P. Kaspi, *J. Chem. Soc. A,* 1873 (1971).
7 C. J. Ballhausen and H. B. Gray, "Molecular Orbital Theory", Benjamin, New York (1965).
8 D. Guenzburger, A. Garnier and J. Danon, *Comptes Rendus Acad. Sc., 273C,* 1205 (1971); *ibid., 274C,* 583 (1972); *ibid., 274C,* 1252 (1972).
9 V. I. Baranovskii, N. V. Ivanova and A. B. Nikol'skii, *Zhurnal Strukturnoi Khimii, 14,* 133 (1973); N. V. Ivanova *et al., Koord. Khim., 1,* 697 (1975) (*C.A., 83,* 87516h).
10 J. R. Durig, W. A. Mc Allister, J. N. Willis Jr. and E. E. Mercer, *Spectrochim. Acta, 22,* 1091 (1966).
11 K. Gleu and I. Büddecker, *Z. anorg. allgem. Chem., 268,* 202 (1952).
12 R. S. Mulliken, *J. Chem. Phys., 23,* 1833 (1955).
13 N. Vannerberg, *Acta Chem. Scand., 20,* 1571 (1966); D. H. Svedung and N. Vannerberg, *Acta Chem. Scand., 22,* 1551 (1968); P. T. Manoharan and W. C. Hamilton, *Inorg. Chem., 2,* 1043 (1963).
14 T. S. Kodashova and G. B. Bokii, *Zhurnal Strukturnoi Khimii, 5,* 250 (1964).
15 T. S. Kodashova, *Zhurnal Strukturnoi Khimii, 6,* 716 (1965).
16 H. Basch and H. B. Gray, *Theoret. Chim. Acta, 4,* 367 (1966).
17 P. T. Manoharan and H. B. Gray, *J. Am. Chem. Soc., 87,* 3340 (1965).
18 E. Clementi, Tables of Atomic Functions, Suppl. to "*Ab-initio* Computations in Atoms and Molecules", *I.B.M. Journal of Research and Development, 9,* 2 (1965).
19 H. Brion, C. Moser and M. Yamazaki, *J. Chem. Phys., 30,* 673 (1959).
20 V. I. Baranovskii and A. B. Nikol'skii, *Theoret. Exp. Chem., 3,* 309 (1970).
21 H. Basch, A. Viste and H. B. Gray, *J. Chem. Phys., 44,* 10 (1966).
22 S. I. Shupack, *Inorg. Chim. Acta, 1,* 435 (1967).
23 J. J. Alexander and H. B. Gray, *Coord. Chem. Rev., 2,* 29 (1967).
24 H. B. Gray and N. A. Beach, *J. Am. Chem. Soc., 85,* 2922 (1963).
25 J. J. Alexander and H. B. Gray, *J. Am. Chem. Soc., 90,* 4260 (1968).
26 H. H. Schmidtke and D. Garthoff, *Helv. Chim. Acta, 49,* 2039 (1966).
27 A. F. Schreiner, S. W. Lin, P. J. Hauser, E. A. Hopcus, D. J. Hamin and J. D. Gunter, *Inorg. Chem., 11,* 880 (1972).
28 J. F. Edincott and H. Taube, *Inorg. Chem., 4,* 437 (1965).
29 T. J. Meyer and H. Taube, *Inorg. Chem., 7,* 2369 (1968).
30 P. Ford, De F. P. Rudd, R. Gaunder and H. Taube, *J. Am. Chem. Soc., 90,* 1187 (1968).
31 D. S. McClure, *Solid State Phys., 9,* 399 (1959).
32 J. Danon and L. Iannarella, *J. Chem. Phys., 47,* 382 (1967).
33 W. Potzel, *Thesis,* Technische Hochschule, München (1970).
34 J. B. Mann, *Rep. L. A.* 3691 (1968).
35 G. M. Bancroft, "Mössbauer Spectroscopy", McGraw-Hill, New York (1973).
36 G. M. Bancroft, K. D. Butler and E. T. Libberg, *J. Chem. Soc. Dalton,* 2643 (1972).